Journal of Pharmaceutical and Biomedical Analysis 54 (2011) 1030–1039

Contents lists available at ScienceDirect

Journal of Pharmaceutical and Biomedical Analysis

journal homepage: www.elsevier.com/locate/jpba

Analysis of triclosan inclusion complexes with β-cyclodextrin and its water-soluble polymeric derivative

Mario Jug[a,*], Ivan Kosalec[b], Francesca Maestrelli[c], Paola Mura[c]

[a] Department of Pharmaceutics, Faculty of Pharmacy and Biochemistry, University of Zagreb, A. Kovačića 1, Zagreb 10000, HR, Croatia
[b] Department of Microbiology, Faculty of Pharmacy and Biochemistry, University of Zagreb, A. Kovačića 1, Zagreb 10000, HR, Croatia
[c] Department of Pharmaceutical Sciences, Faculty of Pharmacy, University of Florence, via Schiff 6, Sesto Fiorentino I-50019, Florence, Italy

ARTICLE INFO

Article history:
Received 17 September 2010
Received in revised form 7 December 2010
Accepted 8 December 2010
Available online 16 December 2010

Keywords:
Triclosan
Cyclodextrin
ROESY
Solid-state analysis
Time–kill analysis

ABSTRACT

Interaction in solution and in the solid state of triclosan (TR), a practically water-insoluble antimicrobial agent, with parent β-cyclodextrin (βCD) and its water-soluble epichlorohydrin polymer (EPI-βCD) was investigated by several analytical techniques, to evaluate the role of the carrier features on the physicochemical properties of the drug–cyclodextrin complex. Phase-solubility studies showed the higher solubilizing and complexing ability of EPI-βCD (K_s = 11,733 M^{-1}) than parent βCD (K_s = 2526 M^{-1}). Actual inclusion complex formation between TR and both cyclodextrins tested was confirmed by 2D ^{1}H NMR studies (ROESY), which also gave insight into some different drug/cyclodextrin binding modes between polymeric and parent βCD. Addition of hydrophilic polymers (hydroxypropylcellulose, hypromellose or amidated pectin) to TR/βCD systems increased βCD solubilizing efficacy, but, unexpectedly, decreased its complexing ability towards the drug. Solid binary and ternary samples prepared by co-grinding of components in high energy mills were carefully characterised by Differential Scanning Calorimetry, X-ray powder diffractometry and Fourier transform infrared spectroscopy. The results pointed out the higher affinity of EPI-βCD than βCD for the interaction with TR even in the solid state, resulting in the formation of completely amorphous products with superior dissolution properties. Addition of hydrophilic polymers failed to effectively promote solid-state interactions between TR and βCD, while their positive influence on drug solubility, observed in phase-solubility studies, was absent in solid TR/βCD/polymer products. Finally, the time–kill analysis, used to evaluate the TR antimicrobial activity against *Streptococcus mutans*, demonstrated the significantly ($p < 0.001$) superior performance of both cyclodextrin complexes than drug alone, and confirmed the higher effectiveness ($p < 0.05$) of TR/EPI-βCD than TR/βCD complex.

1. Introduction

The dental plaque control is an important step in preventing and treating dental diseases such as caries, gingivitis and periodontal diseases, which are by far the most prevalent and diffuse oral conditions worldwide [1]. Numerous clinical studies revealed that this goal may be achieved by regular brushing supported by the use of oral care products containing suitable antimicrobial agents [2].

Triclosan is one of the preferred agents in this field, due to its potent activity against *Streptococcus mutans*, *Streptococcus sanguis*, and *Streptococcus salivarius* and *Actinomycetes* species, that have a major role in aetiology of dental conditions [3]. However, it is practically insoluble in water, which can give rise to formulation problems and reduce or make variable its biological activity [4,5].

Among the different approaches aimed to enhance aqueous solubility of lipophilic drugs, cyclodextrin (CD) complexation proved to be one of the most effective [6–9]. Some of us previously reported that, among natural CDs, triclosan exhibited the highest complexation affinity for parent βCD, but the complex formed was of limited aqueous solubility [4]. The use of hydrophilic βCD-derivatives allowed superior triclosan solubilization and the solubilizing power increased in the order maltosil-βCD < randomly methylated βCD < hydroxypropyl-βCD < sulphobutylether-βCD [10]. However, although the positive effect of different CDs on triclosan aqueous solubility has been shown, the overall solubility achieved by CD complexation is still rather low. All these still lead to unsatisfactory drug bioavailability, especially taking into account its rather short retention time in the oral cavity, when applied in the form of toothpastes and mouthwashes.

Based on these premises, it seemed of interest to extend the range of CDs investigated and evaluate the performance of polymeric CD derivatives. Our approach was based on the superior

* Corresponding author. Tel.: +385 14612608; fax: +385 14612691.
E-mail address: mjug@pharma.hr (M. Jug).

0731-7085/$ – see front matter © 2010 Elsevier B.V. All rights reserved.
doi:10.1016/j.jpba.2010.12.009

solubilizing and complexing ability towards different lipophilic molecules exhibited by polymeric CD derivatives (especially the non-ionic ones), with respect to parent CDs or non-polymeric derivatives [11,12].

In this study we thoroughly investigated the interaction of triclosan with a water-soluble βCD-epichlorohydrin polymer both in solution (by phase solubility and ^{1}H NMR studies) and in the solid state (by thermal analysis, X-ray diffractometry and FTIR spectroscopy) and compared its performance with that of the parent βCD, taken as a reference, in order to gain insight into the role of the carrier features on the physicochemical properties of the final product. The effect of addition of hydrophilic polymers on the CD complexing and solubilizing ability towards triclosan was also evaluated. The dissolution properties of the different binary and ternary drug–carrier solid systems were assessed in simulated saliva solution. Finally, the effect of triclosan complexation with both βCD polymer and parent βCD on its antimicrobial activity against *S. mutans* has been evaluated *in vitro* using the time–kill analysis.

2. Materials and methods

2.1. Materials

Triclosan (TR), 5-chloro-2-(2,4-dichlorophenoxy)-phenol, was kindly donated by Carlo Erba, Italy. β-Cyclodextrin (βCD; Kleptose 4PC) was from Roquette, France, and soluble β-cyclodextrin-epichlorohydrin polymer (EPI-βCD, mean MW 4500) from Cyclolab R&D Ltd., Hungary. Hydrophilic polymers used were hydroxypropyl cellulose (HPC; Klucel EXF, Signet Chemical Corporation Pvt. Ltd., India), low methoxy amidated pectin (AMP; Amid CF 020, Herbstreith & Fox, Germany) and hypromellose (HPMC, Sigma, St. Louis, USA). Deuterium oxide (D_2O; 99.90% purity) was purchased by Sigma (St. Louis, USA). Simulated saliva solution was prepared by dissolving 2.38 g Na_2HPO_4, 0.19 g KH_2PO_4, 8.00 g NaCl in 1 l of distilled water and adjusting pH to 6.75 by the use of orthophosphoric acid. All these products were from Sigma (St. Louis, USA). All other chemicals and solvents used in this study were of analytical reagent grade.

2.2. Methods

2.2.1. Phase-solubility studies

An excess amount of TR (50 mg) was added to 10 mL of simulated saliva (pH 6.75) containing increasing amounts of CD (binary systems). The concentration range for βCD was 0–12.5 mM, while for EPI-βCD was 0–6% (w/v). To evaluate the influence of hydrophilic polymers on TR solubilization by βCD, ternary systems were prepared by adding 1% (w/v) of polymer (HPC, HPMC or AMP) to the TR/βCD binary system. The prepared samples in sealed glass containers were first sonicated 60 min in ultrasonic bath (Eurosonic 44 ultrasonic bath, Wilten Woltil, de Meern, The Netherlands) and then magnetically stirred at constant temperature (25.0 ± 0.5 °C) until equilibrium (72 h). Aliquots were filtered (0.45 μm Millipore membrane filter) and drug concentration was spectrometrically determined at 280.4 nm (Shimadzu 1601 UV-VIS spectrophotometer, Shimadzu Italia S.R.L). Preliminary studies showed that the presence of CDs and polymers did not interfere with TR absorbance at 280.4 nm. Each experiment was repeated at least 3 times (coefficient of variation, C.V. < 2%).

The apparent stability constants of the complexes (K_s) were calculated from the straight portion of the phase-solubility diagrams using Eq. (1) according to Higuchi and Connors [13]:

$$K_s = \frac{\text{slope}}{s_0 \times (1 - \text{slope})} \quad (1)$$

2.2.2. Two dimensional ^{1}H NMR studies (ROESY)

Two-dimensional rotating-frame Overhauser effect spectroscopy (ROESY) was used in order to confirm the actual complexation of TR with the CDs tested, as well as to characterise their binding mode. Since the aqueous solubility of TR was extremely low, it was not possible to obtain its 1D ^{1}H NMR spectrum using D_2O as a solvent. Thus, TR was solubilized by adding an excess amount of drug to 10 mM solutions of βCD or EPI-βCD in D_2O, followed by sample stirring 24 h at 25 °C and final filtration (0.45 μm Millipore membrane filter). The obtained solutions were used to perform 2D ROESY experiments, utilizing a Bruker Avance 400 instrument (Karlsruhe, Germany) operating at 300 K with a 5 mm probe using the standard Bruker parameters (pulse program roesyph) and a mixing time of 350 ms under spin lock conditions at a field of ~2 kHz with TPPI method [14]. The residual HOD signal at 4.70 ppm was used as an internal standard.

2.2.3. Preparation of solid binary systems

Solid binary products of TR with βCD, EPI-βCD or HPC were prepared by co-grinding equimolar drug/CD mixtures or drug/polymer mixture at 10:1 (w/w) ratio in a high-energy vibration micromill (Retsch, GmbH, Germany) at 24 Hz for different times (10, 20, 40, 60 and 80 min). Each time, the degree of drug residual crystallinity was checked by DSC analysis as described in the following section. Physical mixtures (PM) of TR with CD or HPC were prepared by gentle mixing of the accurately weighed components in a mortar with a spatula. To exclude the influence of the sample preparation technique on the physicochemical properties of the drug, pure TR has been treated according to the same grinding procedure, omitting CDs or HPC from the preparation. All samples were kept in desiccator until further analysis.

2.2.4. Preparation of solid ternary systems

Ternary TR/βCD/polymer systems were obtained by adding the polymer to the equimolar drug/CD mixture at 10% (w/w) with respect to TR, followed by co-grinding procedure as described above. The corresponding physical mixture was prepared by gentle mixing of the accurately weighed components in a mortar with a spatula.

2.2.5. Differential Scanning Calorimetry (DSC)

DSC curves of solid products were recorded using a Mettler TA 4000 Star^e apparatus equipped with a DSC 25 cell (Mettler Toledo, Switzerland). The instrument was calibrated with indium and zinc prior to analysis of samples under static air atmosphere. Accurately weighed samples (2–5 mg, Mettler M3 Microbalance) were placed in sealed aluminium pans with pierced lid and scanned at a heating rate of 10 °C min^{-1} over the temperature range of 30–200 °C.

2.2.6. X-ray powder diffractometry (XRPD)

The XRPD spectra were obtained at ambient temperature with a Bruker D8 apparatus (Θ/Θ geometry) using a CuKα radiation and a graphite monochromator. Samples were analysed in the 3–30° 2Θ range, at a scan rate of 0.03° s^{-1}.

2.2.7. Fourier transform infrared spectroscopy (FTIR)

The FTIR spectra of all solid products were recorded by a Perkin-Elmer Model 1600 spectrometer (Wellesley, USA). The samples were prepared by the potassium bromide disc method (3 mg sample in 297 mg KBr) and scanned in the range of 4000–400 cm^{-1} at 2 cm^{-1} resolution.

2.2.8. In vitro dissolution studies

In vitro dissolution studies of the prepared solid products were performed using a modified dispersed amount method according

to the guidelines described by Azarmi et al. [15]. Briefly, a sample amount corresponding to 5 mg of TR was added to 20 mL of simulated saliva solution thermostated at 37 °C and gently stirred (50 rpm) by a magnetic stirrer. At predetermined time intervals, aliquots of 5 mL were withdrawn with a syringe-filter (0.45 μm Millipore membrane filter) and immediately replaced with the same volume of fresh dissolution medium, thermostated at the same temperature. The drug amount in the samples was spectrometrically assayed as described previously. A correction was applied for the cumulative dilution. All experiments were repeated three times for each sample (C.V. < 2.5%).

2.2.9. Determination of Minimal Inhibitory Concentration (MIC) and Minimal Microbicidal Concentration (MMC)

Inocula were prepared by dispersing a fresh culture of *S. mutans* ATCC 33402, cultured on tryptic-soy agar plates (Merck, Germany) with addition of 5% of horse blood during 48 h at 37 °C, in pH 7.4 phosphate buffer up to 0.5 McFarland units (1.5×10^8 CFU mL^{-1}). For this assay, TR and its complexes with both CD tested were previously dissolved in ethanol. MIC and MMC were determined by the twofold micro-dilution method in Müller-Hinton broth (Merck, Germany) in microtiter 96-well plates according to the Clinical and Laboratory Standards Institute (formerly NCCLS) M-27A recommendations [16]. The TR concentration range (both free or as CD complex) was 80–1.25 μg mL^{-1}. The possible antimicrobial effect of both CDs was also tested. MIC was defined as the lowest concentration of tested product that allowed no more than 20% growth of microbes after re-incubation of a 10 μL sample from each dilution on the tryptic-soy agar plate at 37 °C for 48 h. MMC was the lowest concentration which acted as microbicidal, i.e. allowed no growth after sample re-incubation on the tryptic-soy agar plate.

2.2.10. Time–kill analysis

Time–kill analysis was performed in simulated saliva solution (pH 6.75) with *S. mutans* ATCC 33402 as the test strain in the assay. One milliliter of the adjusted inoculum suspension in Müller-Hinton broth of 1 McFarland units (3×10^8 CFU mL^{-1}) was added to 9 mL of simulated saliva solution containing 60 μg mL^{-1} of TR, free of as complex with βCD or EPI-βCD, providing the starting inoculum of 0.3×10^8 CFU mL^{-1}. The culture flasks were incubated at 35 °C. At predetermined time points (0, 1, 2, 4, 6, 8 and 24 h following the addition of investigated products), a 100 μL aliquot was removed from each culture flask and serially diluted in sterile saline. A 100 μL aliquot was plated onto a tryptic-soy agar plate for colony count determination. Plates were then incubated at 35 °C for 48 h. Last two dilutions with growing colonies of *S. mutans* were counted as number of living cells of treated *S. mutans* in time. Time–kill curve was plotted as $\log_{10}$ CFU mL^{-1} of living cells of *S. mutans* treated with prepared products vs. time.

2.2.11. Statistical analysis

Statistical analysis was performed using one-way ANOVA followed by Tukey's multiple comparison test. A p value < 0.05 was considered significant.

3. Results and discussion

3.1. Phase-solubility studies

The TR solubility in simulated saliva solution in the presence of increasing βCD concentrations showed an initial linear increase followed by a plateau region, presenting a B_s type phase-solubility diagram, indicative of the formation of an inclusion complex with limited aqueous solubility [13]. The complex stability constant (Table 1) was considerably higher than the values reported earlier by Másson et al. [17] and Veiga et al. [4] (1400 M^{-1} and 750 M^{-1}, respectively). However, those phase-solubility studies were performed in water, and therefore the observed discrepancy between the results could be explained by the different solubility of TR in simulated saliva and water. Simulated saliva contains high amount of salts, and thus TR solubility was significantly reduced due to salting out effect, thus resulting in a higher K_s value.

Table 1
Parameters obtained by phase-solubility studies of triclosan (TR) with tested cyclodextrins in the presence or absence of 1% hydrophilic polymer.

System	Slope	r^2	K_s (M^{-1})	Solubilizing efficiency[a]
TR/βCD	0.097	0.9989	2526 ± 38[b]	11.5
TR/βCD + 1% HPC	0.062	0.9824	568 ± 19[c]	21.0
TR/βCD + 1% HPMC	0.058	0.9959	523 ± 25[c]	19.1
TR/βCD + 1% AMP	0.085	0.9934	341 ± 8[c]	27.4
TR/EPI-βCD	0.280	0.9955	11,733 ± 40	356.7

[a] Ratio between TR solubility in simulated saliva in binary or ternary systems at the highest CD concentration used and alone.
[b] Significantly different ($p < 0.001$) compared to TR/EPI-βCD.
[c] Significantly different ($p < 0.05$) compared to TR/βCD.

In the attempt to increase the solubilizing efficiency of βCD towards TR, phase-solubility studies were also performed in the presence of a fixed amount (1%, w/v) of a hydrophilic polymer such as HPC, HPMC or AMP. As a consequence of drug–carrier interactions, all the examined polymers alone had some solubilizing effect towards TR, increasing its solubility in simulated saliva from 2.9 times (HPMC) up to 6.4 times (AMP). Interestingly, the addition of the hydrophilic polymers to the βCD complexation medium in all cases gave rise to a change of the phase-solubility diagram from B_s to A_L type, indicative of the formation of soluble complexes [13]

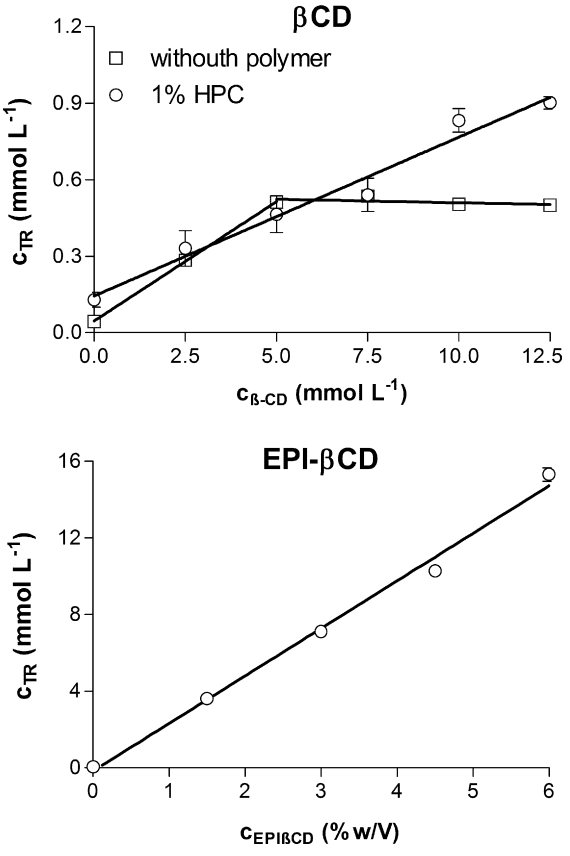

Fig. 1. Phase solubility diagrams of TR and βCD (with or without 1%, w/v of HPC) or EPI-βCD in simulated saliva solution (pH 7.65) at 25 °C.

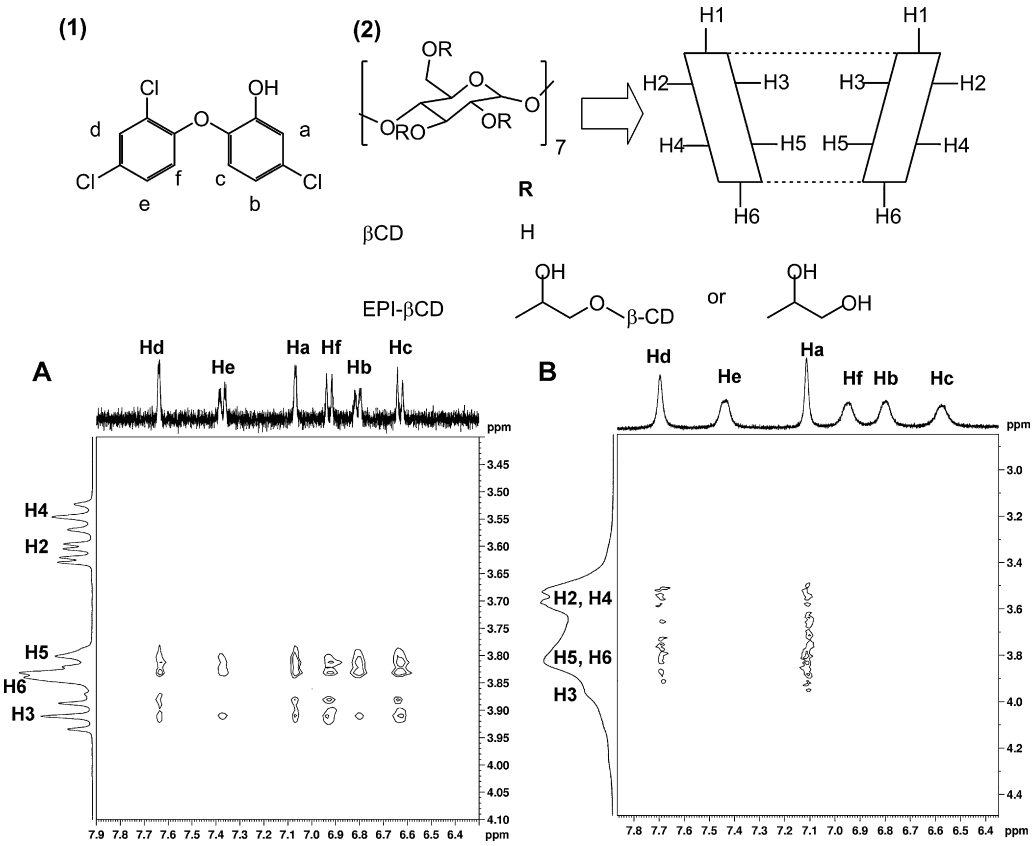

Fig. 2. Partial contour plot of 2D ROESY spectrum of TR in the presence of βCD (A) or EPI-βCD (B) in D_2O at 300 K. The structures and proton labelling of TR (1) and cyclodextrins studied (2) are presented above.

(Fig. 1). However, although the presence of the polymer increased the βCD solubilizing efficiency from 1.7 up to 2.4 times (Table 1), the slopes of the phase-solubility curves and the corresponding K_S values were lower. This indicated that the examined polymers decreased the complexing ability of βCD towards TR, differently from that observed with most of drug–CD–polymer systems, where the hydrophilic polymers presence gave rise to an improvement in the stability constant of drug–CD complexes [18,19]. Possible steric hindrance effects, or the presence of drug–polymer interactions, competing with the drug–CD inclusion complex formation, could be hypothesized to explain the observed reduction of the CD complexing efficacy. Similar results have been reported for ternary systems of TR and other drugs with βCD and chitosan [20,21]. On the other hand, the change of solubility diagram type from B_S (typical of poorly soluble complexes) to A_L (typical of freely soluble complexes) brought about by addition of the examined polymers, seems to indicate that they acted as solubilizer of the TR/βCD complex, thereby giving rise to the increased βCD solubilizing efficiency.

As for the polymeric βCD, TR solubility linearly increased as a function of EPI-βCD concentration, presenting an A_L type solubility diagram (Fig. 1). The stability constant of TR/EPI-βCD complex, calculated by taking the βCD repeating unit as its molecular weight [22], was 4.6 times higher than with the native CD. Moreover, EPI-βCD exhibited a solubilizing efficiency towards the drug more than 30 times higher than the parent βCD (Table 1). Possible formation of micelle like-structures, which could help to explain this result, was excluded by photon correlation spectroscopy (data not shown). Therefore, the high solubilizing power of EPI-βCD towards TR may be attributed to the polymeric structure of this CD derivative, which allowed an efficient cooperation of adjacent CD cavities for interaction with the drug.

3.2. Two dimensional ^{1}H NMR studies (ROESY)

The increased drug solubility in the presence of CD, demonstrated by phase-solubility analysis, cannot be considered as an ultimate proof of the actual inclusion complex formation, and therefore ^{1}H NMR studies were performed. Two-dimensional (2D) ^{1}H NMR is a powerful tool for investigating inter- and intramolecular interactions, since the presence of nOe cross-peaks between the protons from two different species indicates spatial contact within 0.4 nm [23]. Furthermore, it is an effective method to study spatial conformations of CD inclusion complexes [24,25].

The proton labels for TR and CDs studied are presented in Fig. 2. The assignations of ^{1}H chemical shifts of TR, βCD and EPI-βCD were done according to the related literature [14,26–28].

The ROESY spectrum of the TR/βCD sample (Fig. 2A) showed numerous nOe cross-peaks between TR protons and internal protons of βCD (H3 and H5), thus confirming the actual inclusion of the drug molecule into the βCD cavity.

All six TR protons exhibited intermolecular nOe cross-peaks with the internal βCD protons. This may indicate that both TR rings are alternatively inside the βCD cavity, thus implying that two different types of 1:1 inclusion complexes are simultaneously present in solution, as suggested by Paulidou et al. [14]. An alternative explanation could be the complete inclusion of TR molecule into the carrier central cavity, where its rotation/flipping is possible. Furthermore, since nOe cross-peaks were observed for both internal βCD protons, it seems that complex formation occurred by inclusion of the TR molecule via both the wider (H3 part) and the narrower (H5 part) sides of the cone. The simultaneous existence of both binding modes is probably the consequence of the TR molecule geometry. Finally, the presence of complexes of 1:1 stoichiometry in solution was consistent with the findings of

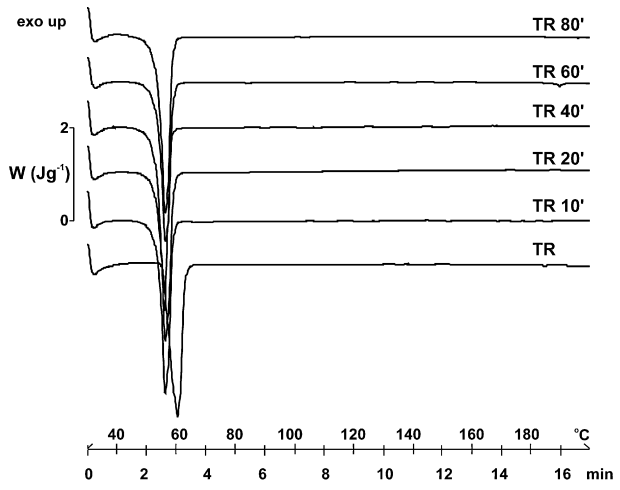

Fig. 3. DSC curves of plain triclosan (TR), untreated and after different grinding times in high-energy mill at 24 Hz.

previous phase-solubility studies, where no positive deviations of the solubility diagram curve were detected, which could be indicative of higher order complexes formation (Ap type according to Higuchi and Connors [13]).

^{1}H NMR spectrum of EPI-βCD was not well resolved. The lack of symmetry due to its completely random polymeric structure, resulted in a ^{1}H NMR spectrum that appeared as several strong and unresolved broad peaks. As a consequence, only some of ^{1}H NMR signals in the EPI-βCD spectrum could be unambiguously identified, while others are uncertain and cannot be used for interpretation of drug inclusion mode. The ROESY spectrum of TR/EPI-βCD sample (Fig. 2B) presented several intermolecular nOe cross-peaks in the 3.5–4.0 ppm area, where signals of the internal (H3 and H5), but also external (H2 and H4) CD protons are expected to be located. The simultaneous interaction with both internal and external EPI-βCD protons may be related to the polymeric structure of this CD. This could probably contribute to explain the higher complexing and solubilizing power of EPI-β-CD towards TR, as emerged by phase-solubility studies. Interestingly, only Hd and Ha protons of TR presented intermolecular nOe cross-peaks with EPI-βCD protons, confirming a different binding mode in comparison with parent βCD.

3.3. Preparation and characterisation of solid samples

Different binary and ternary solid samples of TR with βCD, EPI-βCD and HPC were prepared by co-grinding their mixtures in a high-energy mill. In order to evaluate the effect of different grinding conditions and find the best ones to maximize the interaction between the components, samples were subjected to different milling times and TR decrease in fusion enthalpy, determined by DSC analysis, was assumed as an index of the interaction intensity. Solid-state interactions between the components were further investigated by XRPD and FTIR analyses.

As a first step, to exclude any effect due to the mechanic treatment of samples, TR alone was subjected to the same grinding procedure and the obtained samples were analysed by thermal and spectral analyses. The DSC curve of untreated TR (Fig. 3) presented a sharp endothermic peak at 59.48 °C (ΔH 81.93 J g^{-1}), corresponding to the melting of crystalline drug [4]. After 10 min of milling, the TR fusion peak was shifted to lower temperature (T_{fus} 55.36 °C), with a concomitant slight decrease in fusion enthalpy (ΔH 75.60 J g^{-1}), which may be attributed to a light loss of crystallinity upon milling. However, no further modifications in the drug thermal profile were observed by prolonging the milling time up to 80 min, indicating that the process had only a negligible effect on drug crystallinity.

The XRPD pattern of untreated TR (Fig. 4A) presented several intense peaks at 8.01°, 14.28°, 16.32°, 24.36°, 25.29° and 27.78° 2θ, thus confirming the crystalline nature of the drug [4,3]. The TR sample milled for 80 min presented the same peaks as the initial substance, but their intensity was slightly reduced due to some loss of crystallinity, in agreement with DSC results.

The FTIR spectrum of TR (Fig. 4B) exhibited a peak at 3313 cm^{-1} which corresponds to O–H stretching vibration of phenol hydroxyl group [29]. The intense peaks at 1596 and 1578 cm^{-1} (doublet), 1504 and 1471 cm^{-1} (doublet) and 1417 and 1391 cm^{-1} (doublet) are the consequence of skeletal vibrations, involving C–C stretching inside the benzene ring, while the peaks in the region from 1300 to 1000 and 900 to 650 cm^{-1} correspond, respectively, to in-plane and out-of-plane bending of the aromatic ring C–H bonds [30]. The O–H in-plane bending resulted in several intense peaks in the 1420–1330 cm^{-1} region, while peaks at 1096 and 1089 cm^{-1} correspond to C–Cl absorption. These same peaks with the same intensity were observed in the 80 min TR ground sample, thus confirming that milling procedure did not change the crystal structure of the drug.

The DSC curves of TR mixtures with βCD or EPI-βCD before and after co-grinding procedure for different times are presented in Fig. 5. Both CDs presented thermal curves characterised by the presence of a very broad endothermic band from 40 to 120 °C (ΔH = 156.7 J g^{-1}), associated with water loss. The TR fusion peak was almost unchanged in its physical mixtures with both CDs, indicating the absence of solid-state interaction between the components. On the contrary, the peak intensity gradually decreased as a function of grinding time in co-ground samples and it completely disappeared after 80 min treatment. This indicated that co-grinding procedure was successful to induce effective solid-state interactions between the components, resulting in complete TR amorphization. The amorphous drug state may be indicative of complex formation, because the grinding procedure of drug alone did not have a significant impact on its crystalline properties. Since the drug fusion peak was partially overlapped with the band corresponding to the CD water loss, it was not possible to exactly determine its fusion enthalpy and then calculate the residual TR crystallinity degree at the different co-grinding times. However, while comparing the two series of samples, it may be observed that the decrease of TR fusion peak was more pronounced in its combinations with EPI-βCD, indicating somewhat higher affinity of this CD derivate for the interaction with TR in comparison with βCD, even in the solid state.

The XRPD diagrams of pure drug and CDs, and their equimolar physical mixtures and co-ground samples are presented in Fig. 6.

The βCD diffraction diagram indicated its crystalline nature, while that of EPI-βCD was characteristic of a completely amorphous substance. Diffraction diagrams of equimolar physical mixtures of TR with both CDs tested corresponded to the superposition of plain component diagrams, where all the TR characteristic peaks were still present, confirming the absence of any interaction between the components. The 80 min co-ground sample with βCD still presented some diffraction peaks attributable to TR crystals, even though significantly reduced in intensity compared to the corresponding physical mixture. Thus, DSC behaviour (see Fig. 5) can be explained by assuming that the mechanical treatment led to a highly dispersed microcrystalline TR, making it prone to interact with the carrier by the supply of thermal energy during the DSC scan [31]. Moreover, crystallinity of βCD was also reduced by milling procedure, which may additionally contribute to thermally induced interaction between the components. On the contrary, the TR peaks

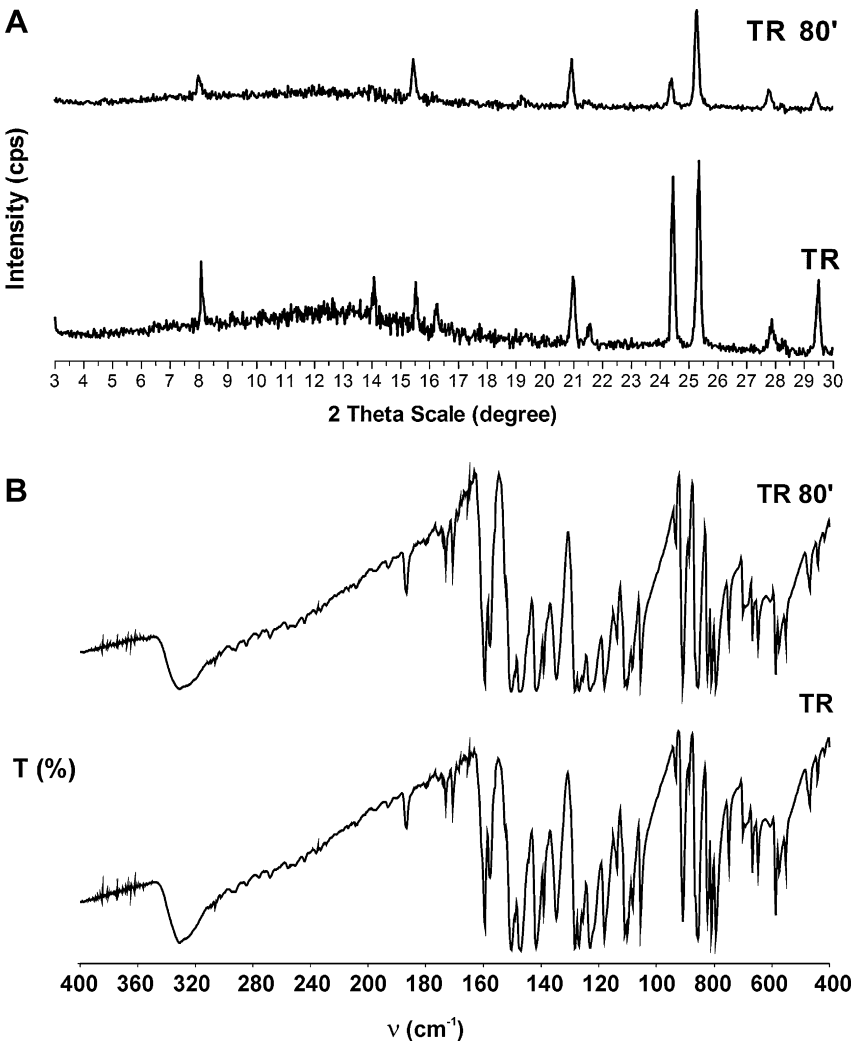

Fig. 4. XRPD diagrams (A) and FTIR spectra (B) of plain triclosan (TR), untreated and after 80 min grinding in high energy mill at 24 Hz (TR 80′).

were completely absent in XRPD pattern of co-ground sample with EPI-βCD, demonstrating the actual complete drug amorphization, probably due to complexation with EPI-βCD. These results were consistent with DSC results and confirmed the superior performance of EPI-βCD than βCD in establishing effective solid-state interactions with the drug.

FTIR analysis further corroborated DSC and XRPD findings (Fig. S1, Supporting information sheet). FTIR spectra of TR equimolar physical mixtures with both CDs tested were the simple superposition of those of pure components and the TR characteristic bands at 1596, 1578, 1504 and 1471 cm^{-1}, attributed to the C–C skeletal vibrations, were well evident, confirming the absence of

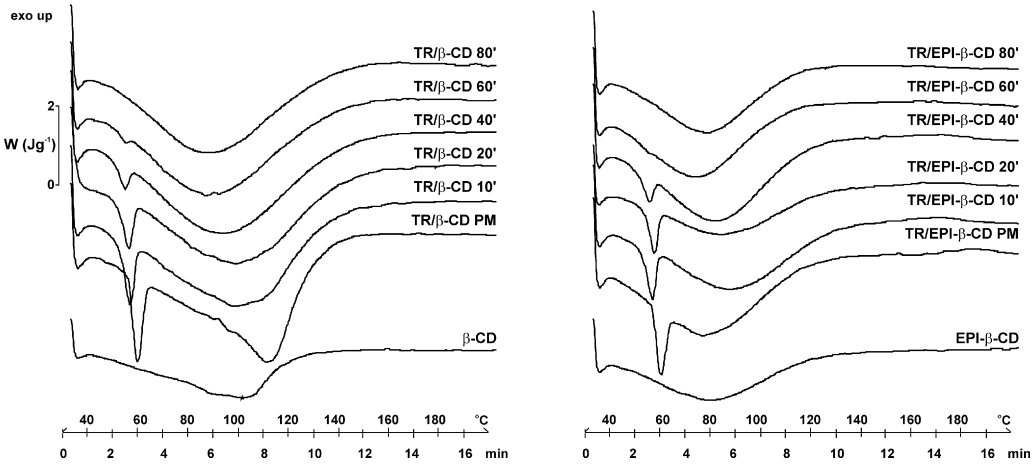

Fig. 5. DSC curves of equimolar samples of TR with βCD of EPI-βCD as physical mixtures (PM) or after different grinding times in high-energy mill at 24 Hz.

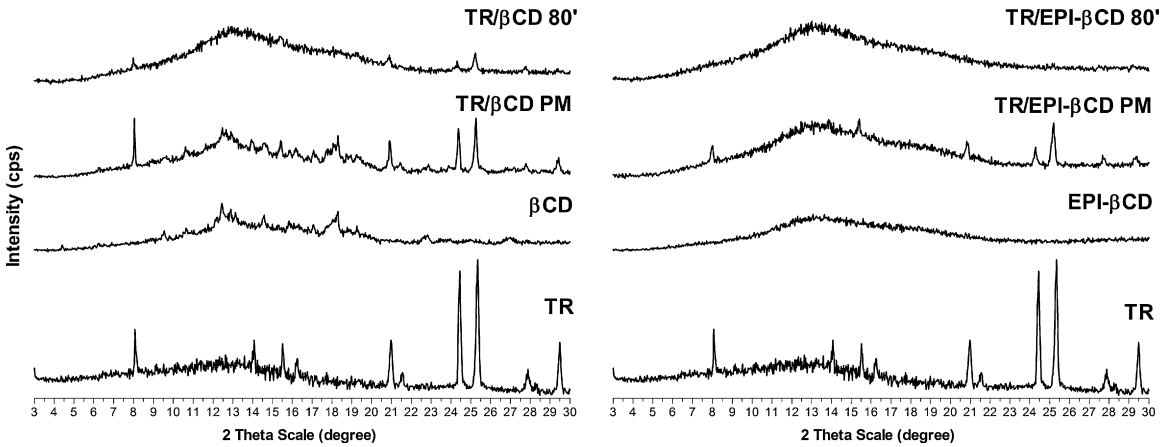

Fig. 6. XRPD diagrams of TR, βCD, EPI-βCD, their equimolar physical mixtures and 80 min co-ground samples in high energy mill at 24 Hz.

significant solid-state interactions. The intensity of TR characteristic absorption bands was considerably reduced in FTIR spectra of 80 min co-ground samples of TR with both CDs, as a consequence of solid-state interactions and/or possible inclusion complex formation [32,33].

Considering the positive results obtained in phase-solubility studies, we considered worthy of interest to evaluate the possible effect of the hydrophilic polymer addition in promoting TR–βCD solid-state interactions. With this aim, a series of drug–polymer and drug–βCD–polymer mixtures (all containing 10%, w/w of polymer with respect to TR) have been prepared and subjected to the co-grinding procedure for different times. The thermal profiles of the series of binary and ternary systems containing HPC are shown in Fig. 7. The DSC curve of HPC, as well as those of the other examined polymers AMP and HPMC, were characterised by a large endothermal effect ranged from 40 to 100–110 °C associated with water loss, typical of their hydrated, amorphous nature.

DSC analysis showed that, in spite of their intrinsically amorphous character, the amorphizing power of the examined polymers towards TR was limited. In fact, even though, the co-grinding time increase gave rise to a progressive reduction of intensity of the drug melting endotherm, this remained always well evident. The drug fusion enthalpy value of the 80-min co-ground sample (53.68 J g^{-1}) showed only a 33% reduction with respect to the starting physical mixture (80.73 J g^{-1}). On the contrary, an analogous reduction in drug fusion enthalpy, in comparison with its corresponding physical mixture, was achieved after only 10-min co-grinding with βCD, despite the crystalline nature of this carrier. As for TR/βCD/HPC ternary systems, only a slight improvement in drug amorphizing efficiency was observed by passing from physical mixtures to co-ground products, with respect to the corresponding binary systems (Fig. 5). Very similar results were obtained also in systems containing AMP or HPMC (data not shown), indicating only a marginal role of the amorphous polymer in promoting more effective drug–CD solid-state interactions.

X-ray diffraction analysis substantially confirmed the DSC results (Fig. 8). In the TR/HPC physical mixture, all TR peaks were still visible, emerging from the amorphous pattern of the polymer, while their intensity was sensibly reduced after 80 min co-grinding. On the other hand, TR characteristic peaks were present also in the diffractogram of the ternary physical mixture, but they almost completely disappeared in the corresponding 80-min co-ground mixture.

The FTIR spectrum of TR/HPC 80-min co-ground sample (Fig. S2, Supporting information sheet) was practically identical to that of the corresponding physical mixture, and no changes were found in the position and intensity of TR characteristic absorption bands. This indicated the absence of any chemical interaction between the components, confirming that the observed partial drug amorphization was a result of the mechanical dispersion of TR particles inside the amorphous HPC matrix.

On the contrary, while comparing the FTIR spectra of TR/βCD/HPC 80-min co-ground product and physical mixture, the almost complete disappearance of TR characteristic absorption

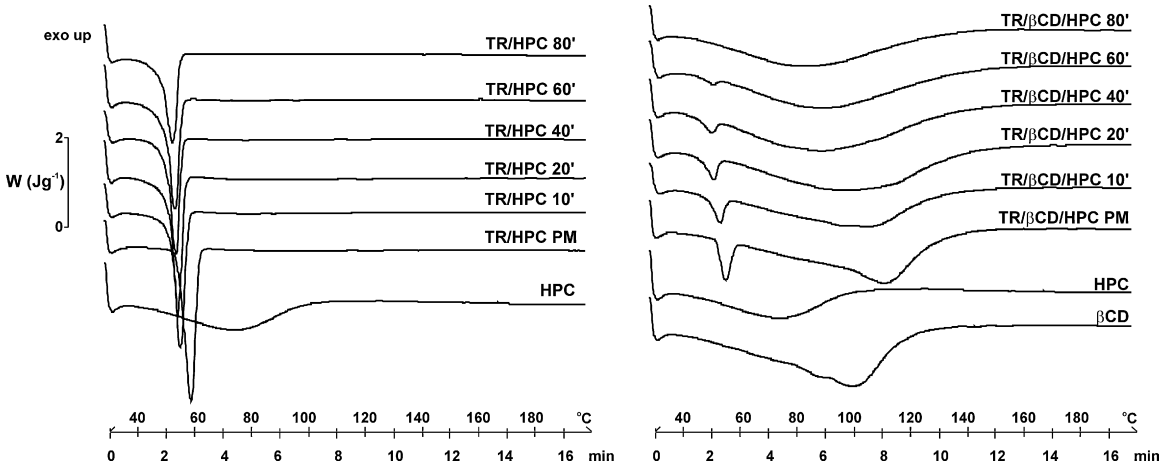

Fig. 7. DSC curves of HPC, binary TR/HPC and ternary TR/βCD/HPC systems as physical mixtures (PM) or after different grinding times in high-energy mill at 24 Hz.

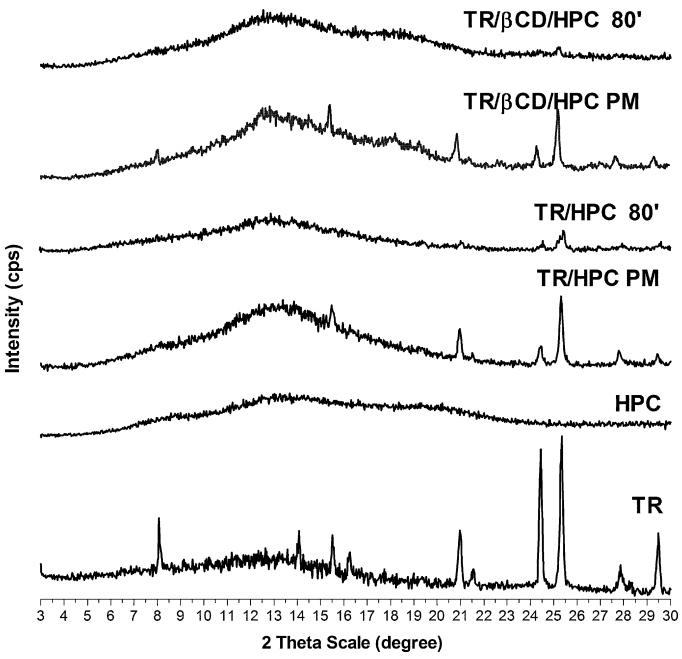

Fig. 8. XRPD diagrams of TR, HPC, and TR/HPC or TR/βCD/HPC systems as physical mixtures (PM) or after 80 min co-grinding in high-energy mill at 24 Hz.

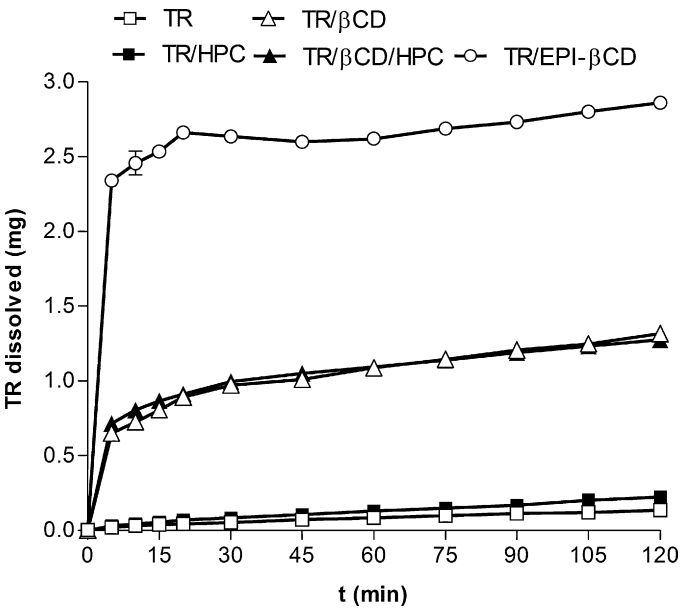

Fig. 9. *In vitro* dissolution profiles of TR alone and from different binary and ternary co-ground systems in simulated saliva solution at 37 °C (mean ± SD).

bands may be observed, as in case of the corresponding TR/βCD binary co-ground system, indicating that the presence of HPC did not interfere in TR/βCD solid-state interactions. Finally, it may be concluded that the higher drug amorphization degree in the case of co-ground ternary sample (Fig. 8) with respect to the binary one (Fig. 6) may be related to simultaneous TR/βCD complex formation and its fine dispersion into the amorphous HPC matrix, promoted by the co-grinding procedure in the high energy mill.

3.4. *In vitro* dissolution studies

In vivo drug dissolution in the oral cavity is hindered by the limited amount of saliva within the mouth and by the presence of an unstirred water layer on its surface. As a consequence, dissolution tests using standard pharmacopeial apparatus, with large volumes of dissolution medium and constant stirring, do not seem to be adequate, because they may give results that cannot reflect the actual *in vivo* dissolution behaviour [15]. In this study a modified dissolution test was used, with reduced volume of dissolution medium, thus better simulating the conditions present at the buccal mucosa. The *in vitro* dissolution profiles of TR alone and from its different binary and ternary co-ground products are shown in Fig. 9.

As expected, the amount of TR dissolved was very low, as a consequence of its very poor aqueous solubility. After 120 min, only 2.7% of the drug dose was dissolved. The TR/HPC co-ground product presented a somewhat improved dissolution profile, resulting in dissolution of approximately 4.4% of the dissolved TR dose upon 120 min. This slight but statistically significant ($p < 0.05$) improvement may be related to the drug decreased crystallinity upon co-grinding with HPC, as demonstrated by DSC and XRPD analyses, and to some polymer solubilizing effect. In case of TR–βCD co-ground system, the amount of dissolved drug after 5 min was 13% of applied dose, and it reached 26.3% after 120 min, which was significantly higher compared to both TR alone and TR-HPC co-ground product ($p < 0.01$). Surprisingly, the ternary TR/βCD/HPC co-ground product exhibited practically the same dissolution profile as the TR/βCD binary one ($p > 0.05$), indicating that the presence of HPC failed to additionally increase the drug dissolution rate. This effect may be associated with the absence of ternary complex formation, as discussed previously. Furthermore, the lack of the polymer solubilizing effect towards the TR/βCD complex, observed in phase-solubility studies (Fig. 1), can be attributed to the different experimental conditions of dissolution test. In fact, in this case, the concurrent dissolution of all components of the solid TR/βCD/HPC co-ground product probably resulted in some competition between the TR/βCD complex and the polymer for the hydration/dissolution process. This effect was particularly evident due to the limited amount of dissolution medium and the limited stirring conditions used to simulate the oral cavity situation.

The dissolution profile of TR/EPI-βCD presented instead a very fast initial phase, resulting in dissolution of approximately 50% of the drug dose in first 5 min, followed by a plateau after 30 min. After 120 min, approximately 60% of TR initial dose was dissolved, thus confirming the superior performance of EPI-βCD in comparison with the parent βCD ($p < 0.001$) in improving drug dissolution properties, which is consistent with phase-solubility studies.

3.5. *Effect of CD complexation on triclosan antimicrobial activity against S. mutans*

Microdilution assay showed that MIC of TR, free or as complex with βCD or EPI-βCD, was 5 μg mL^{-1}, while MMC was 10 μg mL^{-1}, irrespective of the CD presence or not. This indicated that CD complexation of the drug did not interfere with its antimicrobial activity against *S. mutans*. Furthermore, in the same test, both CDs alone did not present any antimicrobial activity against *S. mutans*.

The antimicrobial activity of the prepared products was also tested using the time–kill methodology. Klepser et al. [34] demonstrated the ability of this methodology as an indispensable tool for assessing the activity of antimicrobials against bacteria. In fact this approach allows the estimation of drug antimicrobial activity as a function of time, which could be a more accurate determinant for clinical outcome of therapy than a simple numerical MIC or MMC [35]. Moreover, this kind of test can be particularly relevant for drugs with poor solubility and short “in situ” application times such as TR.

The time–kill curves for TR alone or as complex with βCD and EPI-βCD are presented in Fig. 10. It is important to point out that in this test TR and its CD complexes were added to the culture medium

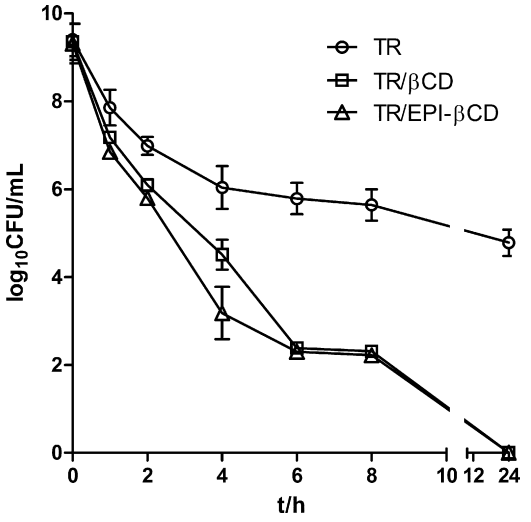

Fig. 10. Time–kill curves of *S. mutans* treated with TR alone or as complex with βCD or EPI-βCD (mean ± SD, $n = 3$).

as solids, while in the microdilution assay they were previously dissolved in concentrated ethanol.

TR alone, although it was added to the test medium in concentration 6 times higher than its MMC, reduced the number of bacteria only for $2 \log_{10}$ CFU mL^{-1}. This clearly indicated that the very low solubility of TR in simulated saliva is a serious hindrance for its antimicrobial activity, i.e. its low solubility does not allow achievement of MIC and MMC concentration in the medium. This may lead to lack of therapeutic activity *in vivo*. Both complexes on the other hand showed superior performance in respect to drug alone ($p < 0.001$) at all time points (Fig. 10), resulting in complete eradication of *S. mutans* after 24 h of incubation. This may be directly related to improved solubility of TR upon complexation, since only dissolved drug would be able to target the bacteria and to reveal its pharmacological action. Moreover, in aqueous environment, cyclodextrin would act as a carrier, by transporting the drug molecule across the hydrophilic media. At the bacteria surface, a partition of the drug from CD complex to the bacteria lipophilic membrane would occur, so making the drug available to perform its pharmacological action.

During the first 4 h, TR complex with EPI-βCD demonstrated somewhat better performance in comparison to βCD complex ($p < 0.05$), which may be attributed to greater solubility of this complex than that with parent βCD, as demonstrated by dissolution studies (Fig. 9). After this period, both complexes showed comparable time–kill curves ($p > 0.05$). From time–kill assay it may be concluded that EPI-βCD is a derivative of choice for preparation of formulations aimed for local delivery of TR into the oral cavity. In fact, besides its higher solubilizing efficiency against the drug, its non-ionic nature would lead to low probability of incompatibilities with formulation components. Finally, the significance of EPI-βCD as carrier for TR is even more important, taking into account that cationic βCD polymer failed to enhance antimicrobial efficiency of TR, as reported by Quan et al. [29].

Acknowledgments

Financial support from MIUR and a personal Post doctoral grant to M. Jug from the National Foundation for Science, Higher Education and Technological Development of the Republic of Croatia are greatly acknowledged.

Appendix A. Supplementary data

Supplementary data associated with this article can be found, in the online version, at doi:10.1016/j.jpba.2010.12.009.

References

[1] R.C. Oliver, L.J. Brown, H. Löe, Peridontal diseases in the United State population, J. Peridontol. 69 (1998) 269–278.
[2] P. Gilbert, A. McBain, P. Sreenivasan, Common therapeutic approaches for the control of oral biofilms: microbiological safety and efficiency, Clin. Microbiol. Infect. 13 (2007) 17–24.
[3] A. Dinge, M. Nagaresenker, Formulation and evaluation of fast dissolving films for delivery of triclosan to the oral cavity, AAPS Pharm. Sci. Tech. 9 (2008) 349–356.
[4] M.D. Veiga, M. Merino, M. Cirri, F. Maestrelli, P. Mura, Comparative study on triclosan interactions in solution and in the solid state with natural and chemically modified cyclodextrins, J. Incl. Phenom. Macrocyclic Chem. 53 (2005) 77–83.
[5] S.I. Stratul, D. Onisei, D. Rusu, Antimicrobial agents in periodontal disease therapy: rationale and use of the triclosan PVM/MA copolymer in the management of gingivitis. Data from a consensus report. Part I, TMJ 59 (2009) 105–108.
[6] T. Loftsson, M.E. Brewster, M. Másson, Role of cyclodextrin in improving oral drug delivery, Am. J. Drug Deliv. 2 (2004) 261–275.
[7] S. Tommasini, D. Raneri, R. Ficarra, M.L. Calabrò, R. Stancanelli, P. Ficarra, Improvement in solubility and dissolution rate of flavonoids by complexation with β-cyclodextrin, J. Pharm. Biomed. Anal. 35 (2004) 379–387.
[8] H.A. Hassan, A.H. Al-Marzouqi, B. Jobe, A.H. Hamza, G.A. Ramadan, Enhancement of dissolution amount and in vivo bioavailability of itraconazole by complexation with β-cyclodextrin using supercritical carbon dioxide, J. Pharm. Biomed. Anal. 45 (2007) 243–250.
[9] R. Grillo, N.F.S. De Melo, C. Morales Moraes, R. de Lima, C.M.S. Menezes, E.I. Ferreira, A.H. Rosa, L. Fernandes Fraceto, Study of the interaction between hydroxymethylnitrofurazone and 2-hydroxypropyl-β-cyclodextrin, J. Pharm. Biomed. Anal. 47 (2008) 295–302.
[10] T. Loftsson, N. Leeves, B. Bjornsdottir, L. Duffy, M. Masson, Effect of cyclodextrin and polymers on triclosan availability and substantivity in toothpastes in vivo, J. Pharm. Sci. 88 (1999) 1254–1258.
[11] L. Szente, J. Szejtli, Highly soluble cyclodextrin derivatives: chemistry, properties, and trends in development, Adv. Drug Deliv. Rev. 36 (1999) 17–28.
[12] A.M. Layre, N.M. Gosselet, E. Renard, B. Sebille, C. Amiel, Comparison of the complexation of cosmetical and pharmaceutical compounds with γ-cyclodextrin, 2-hydroxypropyl-β-cyclodextrin and water soluble β-cyclodextrin-co-epichlorohydrin polymers, J. Incl. Phenom. Macrocyclic Chem. 43 (2002) 311–317.
[13] T. Higuchi, K. Connors, Phase solubility techniques, Adv. Anal. Chem. Instrum. 7 (1965) 117–212.
[14] A. Paulidou, D. Maffeo, K. Yannakopoulou, I.M. Mavridis, Crystal structure of the inclusion complex of the antibacterial agent triclosan with cyclomaltoheptaose and NMR study of its molecular encapsulation in positively and negatively charged cyclomaltoheptaose derivates, Carbhoydr. Res. 343 (2008) 2634–2640.
[15] S. Azarmi, W. Roa, R. Löbenberg, Current perspectives in dissolution tests of conventional and novel dosage forms, Int. J. Pharm. 328 (2007) 12–21.
[16] National Committee for Laboratory Standards (NCCLS), Reference Method for Broth Dilution Antifungal Susceptibility of Yeasts, Approved Standards M27-A, National Committee for Laboratory Standards, Wayne, PA, 1997.
[17] M. Másson, B.V. Sigurdadóttir, K. Matthíasson, T. Loftsson, Investigation of drug–cyclodextrin complexes by a phase distribution method: some theoretical and practical considerations, Chem. Pharm. Bull. 53 (2005) 958–964.
[18] T. Loftsson, H. Fridriksdottir, The effect of water-soluble polymers on the aqueous solubility and complexing abilities of β-cyclodextrin, Int. J. Pharm. 163 (1998) 115–121.
[19] M.T. Faucci, P. Mura, Effect of water-soluble polymers on naproxen complexation with natural and chemically-modified-β-cyclodextrins, Drug Dev. Ind. Pharm. 27 (2001) 311–319.
[20] F. Maestrelli, M. Garcia-Fuentes, P. Mura, M.J. Alonso, A new drug nanocarrier consisting of chitosan and hydroxypropylcyclodextrin, Eur. J. Pharm. Biopharm. 63 (2006) 79–86.
[21] P. Mura, G. Corti, F. Maestrelli, M. Cirri, The influence of chitosan on cyclodextrin complexing and solubilizing abilities towards drugs, J. Incl. Phenom. Macrocyclic Chem. 59 (2007) 307–313.
[22] P. Mura, M.T. Faucci, F. Maestrelli, S. Furlanetto, S. Pinzauti, Characterization of physicochemical properties of naproxen systems with amorphous β-cyclodextrin–epichlorohydrin polymers, J. Pharm. Biomed. Anal. 29 (2002) 1015–1024.
[23] H.J. Schneider, F. Hacket, F.V. Rüdiger, H. Ikeda, NMR studies and cyclodextrin complexes, Chem. Rev. 98 (1998) 1755–1785.
[24] M.V.G. de Araújo, E.K.B. Vieira, G.S. Lázaro, L.S. Conegero, L.E. Almeida, L.S. Barreto, N.B. da Costa, I.F. Gimenez, Sulfadiazine/hydroxypropyl-β-cyclodextrin host–guest system: characterization, phase-solubility and molecular modeling, Bioorg. Med. Chem. 16 (2008) 5788–5794.
[25] C. Julian, T. Ortosteguis, P. Pérez-Cruz, F. Sáánchez, C. Mendizabal, Olea-Azar, Complexation of morin with tree kinds of cyclodextrin. A thermodynamic and reactivity study, Spectrochim. Acta A 71 (2008) 269–275.

[26] M. Duan, N. Zhao, I. Őssurardóttir, T. Thorsteinsson, T. Loftsson, Cyclodextrin solubilization of the antibacterial agents triclosan and tricarban: formation of aggregates and higher-order complexes, Int. J. Pharm. 297 (2005) 213–222.
[27] S. Gibaud, S.B. Zirar, P. Mutzenhardt, I. Fries, A. Astier, Melarsoprol–cyclodextrin inclusion complexes, Int. J. Pharm. 306 (2005) 107–121.
[28] J. Li, H. Xiao, J. Li, Y.P. Zhong, Drug carrier systems based on water-soluble cationic β-cyclodextrin polymers, Int. J. Pharm. 278 (2004) 329–342.
[29] L. Quan, Y. Guan, H. Xiao, Preparation and characterization of inclusion complexes of a cationic β-cyclodextrin polymer with butylparaben or triclosan, Int. J. Pharm. 357 (2008) 244–251.
[30] S.M. Iconomopoulou, A.K. Andreopulou, A.J. Soto, K. Kallitsis, G.A. Voyiatzis, Incorporation of low molecular weight biocides into polystirene-divinyl benzene beads with controlled release characteristics, J. Control. Release 102 (2005) 223–233.
[31] P. Mura, G.P. Bettinetti, M.T. Faucci, M. Sorrenti, A. Negri, Interaction of naproxen with crystalline and amorphous methylated-β-cyclodextrin in the liquid and solid state, Supramol. Chem. 12 (2001) 379–389.
[32] O. Aleem, B. Kuchenkar, Y. Pore, S. Late, Effect of β-cyclodextrin and hydroxypropylβcyclodextrin complexation on physicochemical properties and antimicrobial activity of cefdinir, J. Pharm. Biomed. Anal. 47 (2008) 535–540.
[33] W. Misiuk, M. Zalewska, Investigation of inclusion complexes of trazodone HCl with hydroxypropylβcyclodextrin, Carbohydr. Polym. 77 (2009) 482–488.
[34] M.A. Klepser, E.J. Ernst, L.E. Lewis, M.A. Pfaller, Influence of test conditions on antifungal time–kill curve results: proposal for standardized methods, Antimicrob. Agents Chemother. 42 (1998) 1207–1212.
[35] M.C.S.M. Pappalardo, M. Walderez Szesz, M.A. Martins, L.B. Baceti, L.X. Bonfietti, S.U. Purisco, A.A. Baez, M.S.C. Melhem, Susceptibility of clinical isolates of Cryptococcus neoformans to amphotericin B using time–kill methodology, Diagn. Microbiol. Infect. Dis. 64 (2009) 146–151.